ABSTRACT

Title of Thesis: SYNCHRONIZED SWIMMING AND FORMATION CONTROL FOR FISH-INSPIRED UNDERWATER VEHICLES

Paul Ghanem
Master of Science in Systems Engineering 2019

Thesis directed by: Professor Derek A. Paley
Department of Aerospace Engineering

Multi-vehicle underwater control has different applications in oceanographic sampling and water pollution monitoring. Previous work in this field generated control laws that stabilizes parallel and circular formations of self-propelled particles in addition to consensus control laws in Euclidean space and nonlinear spaces. This thesis presents second order distributed control systems that generate velocity and phase consensus, parallel motion and circular motion for a number of nonlinear agents on the tangent bundle of the N-torus. The nonlinear agents considered in this work are underwater fish inspired vehicles modeled by Chaplygin sleigh dynamics. This work uses the Laplacian matrix of a connected interaction graph to achieve phase and velocity consensus on a periodic orbit and to generate average circular motion of all the agents on the same circle. Second, a phase potential is used to generate average parallel motion. Results are illustrated using numerical simulations.

SYNCHRONIZED SWIMMING AND FORMATION CONTROL FOR FISH-INSPIRED UNDERWATER VEHICLES

by

Paul Ghanem

Thesis submitted to the Faculty of Engineering of the Graduate School of the
University of Maryland, College Park in partial fulfillment
of the requirements for the degree of
Master of Science
2019

Advisory Committee:
Professor Advisor Derek Paley, Chair
Professor Nikhil Chopra
Professor Mumu Xu

Acknowledgments

I would like to take the opportunity to thank people who helped me in my journey at the University of Maryland. In particular, I want to thank Professor Derek A. Paley for giving me the opportunity to work in the Collective Dynamics and Control Laboratory. This work would not be completed without his thorough advice and insightful suggestions. I would also like to acknowledge Artur Wolek for his guidance in writing the Thesis document. In addition, I would like to thank Brian Free and Jinseong Lee for designing the fish and sharing information about its behavior. I am grateful for the members of the Collective Dynamics and Control laboratory for I am very proud to work alongside such exceptional people.

Finally, I want to thank everyone who helped me in my academic career starting from Lebanon, in particular Professor Samer Saab who I would not be at this stage without his support.

To the memory of my friend $\boldsymbol{Zakhia\ Rahi}$,

to my parents $\boldsymbol{Joseph}$ and $\boldsymbol{Jeanne\ D'arc}$,

to my brother $\boldsymbol{Elias}$ and my sister $\boldsymbol{Hanane}$.

Table of Contents

List of Tables

List of Figures

Chapter 1: Introduction

1.1 Motivation for Research

The motivation for researching collective behavior of autonomous underwater vehicles originates from the growing need to estimate rapidly evolving spatio-temporal processes using mobile sensor network. For example, a collection of underwater vehicles performing oceanographic sampling can further the understanding of the effect of ocean water quality on ocean streams. Similarly, a coordinated collection of vehicles doing underwater pipeline inspection can decrease the risk of problems and pipeline pollution. For this reason, collective behavior of mobile agents has received significant interest recently in various fields such as biology, physics, computer science, and control engineering [1], [2], [3]. Research in this area is allowing scientists to better understand swarming behavior in nature and benefits control engineers in various applications by mimicking nature's behavior in engineered mobile systems such as unmanned ground, air, and underwater vehicles. Various swarming techniques have been studied and applied such as flocking, formation, and consensus control which happens when the vehicles reach an agreement on their collective direction, heading, velocity or any other vehicle state [4], [5], [6]. While these swarming techniques are important for vehicle coordination during a task, existing consensus and formation control algorithms considered driv-

ing the vehicles state variables to be non-oscillating, where an oscillating state variable is an agent state variable that oscillates around a point, which is not always realistic and sometimes undesired. Therefore, there is a need for a swarming algorithm that consider driving the agents to formation or consensus control with oscillating state variables to enable applications requiring more complex coordination.

1.2 Relation to Previous work

Consensus control in Euclidean space, which assumes that the state variables of the system live on $\mathbb{R}^N$, is a well-studied topic [7]. The goal of consensus control is to steer N agents into identical state variables, where heading an angular velocity of an agent is an example of a state variable. For example, consensus control is used for rendezvous [8] and formation control [9], [10]. Consensus is typically studied for single-integrator dynamics [11], [12], which could contain linear or nonlinear drift vector fields [13], [14]. Interactions between agents can be static [15], time-varying [11], [12], all-to-all [15] or limited [16]. These interactions are typically described using the Laplacian matrix from algebraic graph theory [17] to compute relative state information, such as relative position.

Euclidean consensus has also been studied for double-integrator dynamics [18]. In this setting, most prior work uses feedback of relative position and velocity [19], [20], [21]. Second-order Euclidean consensus is possible for systems with a nonlinear drift vector field that represents the vehicle dynamics [21]. The presence of a virtual leader permits vehicles to follow a desired trajectory [20].

Consensus control on a nonlinear manifold has also been studied previously [22], [23], [24], [25], [26]. For example, consensus on the N-torus—also called synchronization—arises in the control of planar formations, where the heading orientation is a phase angle on the unit circle [27]. Orientation and translation control of agents in the plane utilizes the special Euclidean group [28]. Many synchronization approaches [29], [30] are based on principles from the theory of coupled oscillators, such as the celebrated Kuramoto model [27], and invoke the graph Laplacian for cooperative control of first-order dynamics on the N-torus [31]. Second-order consensus of coupled oscillators with double-integrator dynamics [32] uses the gradient of a phase potential. However, no previous work on consensus considers second-order oscillators with nonlinear dynamics.

Similarly, circular formation control for first order dynamics on the N torus has also been studied in [25]. an extension to [25] was done in [32] where circular formation was achieved on tangent bundle of the N-torus. Nevertheless, none of the previous work accounted for vehicle dynamics and motion requirements of each agent.

1.3 Technical Approach

In this thesis, I extend the different consensus, synchronization and circular formation control approaches that were done on different topologies, such as the Euclidean space $\mathbb{R}^N$ and the N- torus $\mathbb{T}^N$, using first order and second order integrator dynamics. I extend these control approaches to incorporate the tangent bundle of the N- torus and the dynamics of a fish robot designed in the Collective Dynamics and Control laboratory. The motion of the robotic fish [33] is modeled by the Chaplygin sleigh dynamics.

These dynamics are simplified using single-perturbation method to facilitate the design and analysis of a swarm controller that is inspired by the self propelled particle model in [25].

1.4 Contributions of Thesis

The first contribution of this thesis is a tracking controller for a single Chaplygin sleigh fish by convergence to a desired limit cycle, where the heading of the fish oscillates around a desired trajectory while tracking it on average.

A second contribution is thesis second-order consensus control law for multiple phase oscillators with a nonlinear drift vector field. The proposed controller requires only relative velocity measurements, rather than relative position and velocity, computed using the Laplacian matrix of a connected interaction graph. The heading and angular velocity reach consensus on a periodic orbit, where the value of the heading and angular velocity of each fish is oscillating. As a sub-contribution, the consensus control is illustrated for the case of a system of nonlinear oscillators representing the closed-loop swimming dynamics of a school of robotic fish [33]. The individual fish-robot dynamics are represented by the Chaplygin sleigh [34], [33], which is a nonholonomic mechanical system, propelled by an internal rotor.

Another contribution of this thesis is average phase synchronization for multiple phase oscillators on the N-torus with a nonlinear vector field, which as before, is the Chaplygin sleigh dynamics of the fish. The control law does not include a virtual leader or a desired direction of motion to track. Consensus in this case is reached on average for

the same heading and angular velocity, that varies along a periodic orbit.

The final contribution of this thesis is circular formation control on the tangent bundle of the N-torus for multiple phase oscillators with a nonlinear vector field. The vehicles are stabilized on the same circle while maintaining an oscillating angular velocity.

1.5 Outline of Thesis

The remainder of this thesis is organized as follows. Section 2 provides preliminaries on graph theory, defines the consensus problem on the tangent bundle of the N-torus, and the first and second order self propelled particle models. Section 3 presents the Chaplygin sleigh fish with control algorithms that achieve single fish straight and circular motion. Section 4 presents a general formulation of the consensus result for second-order oscillators with nonlinear dynamics and applies the general result to the Chaplygin sleigh dynamics. Section 5 develops the phase synchronization and circular formation control algorithms on the Chaplygin sleigh swarm. Section 6 summarizes the thesis and discusses ongoing work.

Chapter 2: Background

2.1 Graph Theory

A graph is used to represent the communication topology of an interacting system of agents. The communication graph is built upon a set of nodes $\mathcal{N} = \{1, \ldots, N\}$ that represents the agents. An edge denoted by the pair (i, j) exists between agent $i \in \mathcal{N}$ and $j \in \mathcal{N}$ if information flows from j to i. The set of all edges is denoted $E \subseteq \mathcal{N}^2$. Together, the set of nodes $\mathcal{N}$ and the edges E define a graph $G = (\mathcal{N}, E)$ [35]. A sequence of edges $\{(i, i_1), (i_1, i_2), \cdots, (i_l, j)\}$ with distinct nodes $i_k \in \mathcal{N}$, $i_k \neq i, i_k \neq j$, for $k = 1, 2, \cdots, l$ is called a path from node i to node j. A graph G is called undirected if $(i, j) \in E$ if and only if $(j, i) \in E$. If there exists a path between any pair of distinct nodes $i, j \in \mathcal{N}$, an undirected graph G is called connected. Edges are expressed using the adjacency matrix $A \in \mathbb{R}^{N \times N}$, where the entry on the ith row and jth column is

$$A_{ij} = \begin{cases} 1 & \text{if} \quad (i, j) \in E \\ \\ 0 & \text{otherwise} \end{cases}.$$

The degree matrix $D \in \mathbb{R}^{N\times N}$ encodes how many unique edges are connected to each node and has nonzero elements on the diagonal, i.e.,

$$D_{ij} = \begin{cases} \sum_{k=1}^{N} A_{ik} & \text{if} \quad i = j \\ 0 & \text{otherwise} \end{cases} .$$

The symmetric and positive semi-definite Laplacian matrix $L \in \mathbb{R}^{N\times N}$ associated with the undirected graph G is

$$L = D - A \, . \tag{2.1}$$

The Laplacian matrix is used to compute relative state information that is communicated between agents. The quadratic form $\boldsymbol{x}^T L \boldsymbol{x} \geq 0$, where $\boldsymbol{x} \in \mathbb{R}^N$ may represent a state of interest, is equal to zero if and only if $x_i = x_j, \forall \, i, j \in \mathcal{N}$.

2.2 Consensus and Synchronization

This thesis considers a fixed undirected network $G = (\mathcal{N}, E)$ composed of N identical agents with the following second-order nonlinear dynamics:

$$\dot{\theta}_k = \omega_k \tag{2.2}$$

$$\dot{\omega}_k = g(\omega_k) + u_k(\boldsymbol{\theta}, \boldsymbol{\omega}) \, , \tag{2.3}$$

where $\boldsymbol{\theta} = \{\theta_1, \cdots, \theta_N\} \in \mathbb{T}^N$ is the set of agent phase angles on the N-torus $\mathbb{T}^N \triangleq \{\mathbb{S}^1 \times \cdots \times \mathbb{S}^1\}$, $\boldsymbol{\omega} = \{\omega_1, \cdots, \omega_N\} \in \mathbb{R}^N$ is the corresponding set of angular rates, $g(\omega_k)$ represents the (nonlinear) dynamics of agent k, and $u_k(\boldsymbol{\theta}, \boldsymbol{\omega})$ is the state-feedback control

input to agent k. The tangent bundle on the N-torus is the disjoint union of tangent spaces $T_p\mathbb{T}^N$ for all points p on the N-torus [36].

Definition 1. *The problem of second-order consensus on the tangent bundle of the N-torus for the system (2.2),(2.3) is to design a control input u_k for $k \in \mathcal{N}$ such that*

$$\lim_{t\to\infty} \|\theta_k - \theta_j\| = 0 \tag{2.4}$$

$$\lim_{t\to\infty} \|\omega_k - \omega_j\| = 0 \ , \tag{2.5}$$

for all pairs $k, j \in \mathcal{N}$.

Note that ω_k does not necessarily converge to zero. In fact, we are interested in the case where (θ_k, ω_k) forms a limit cycle for all $k \in \mathcal{N}$.

2.3 Self-Propelled Particle Dynamics and Cooperative Control

In our study of swarm behavior, parallel and circular formation of self propelled particles are used as the basis of more complex motion. Hence, in order to understand the control laws of the following chapters, the first and second order particle models are described here. The corresponding control inputs that achieve circular and parallel motion are also reviewed.

In the self propelled particle model, the position of the kth particle with respect to the origin of the inertial frame is $r_k \in \mathbb{C}$ where $k \in \mathcal{N}$. The velocity of the kth particle is the time-derivative, with respect to the inertial frame, of the position. That is, $\dot{r}_k = \frac{d}{dt} r_k$. The velocity of each particle in polar coordinates is expressed as $\dot{r}_k = s_k e^{i\theta_k}$, where s_k

is the speed and θ_k is the direction of motion of particle k. $\theta_k \in \mathbb{T}$ is called the phase of particle k where $\mathbb{T}$ is the torus. The torus here is the same as the circle $\mathcal{S}^1 \triangleq [0, 2\pi)$ and the N-torus $\mathbb{T}^N \triangleq S^1 \times .. \times S^1$ (N times).

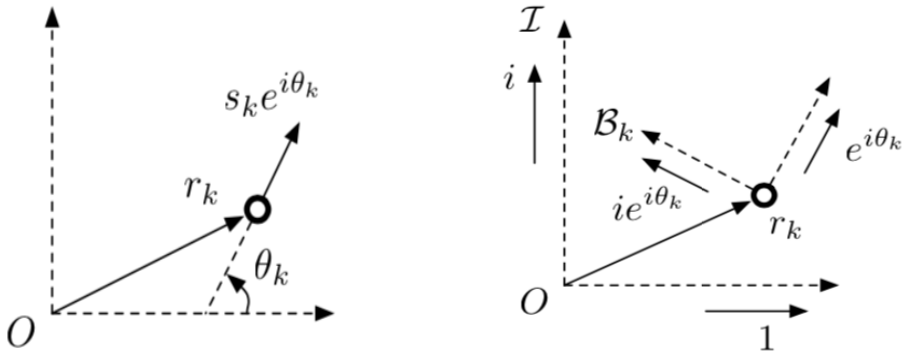

(a) Coordinates (b) Reference frame

Figure 2.1: Planar particle dynamics: Each particle is modeled as a self propelled particle with position r_k, speed s_k and phase θ_k.

In [25], a self propelled particle model with first order steering was used to design collective motion. The particle model assumes that all particles have a unit constant speed $s_k = 1$ and all-to-all communication between agents.

Let N denote the number of particles. Let $r_k \in \mathbb{C}, \theta_k \in \mathbb{T}$ and $u_k \in \mathbb{R}$ denote the position, phase and steering control for particle $k \in \mathcal{N}$, where $\mathcal{N} = [1, ..., N]$ respectively. The particle model with first order steering becomes:

$$\begin{aligned} \dot{r}_k &= e^{i\theta_k} \\ \dot{\theta}_k &= u_k \end{aligned} \tag{2.6}$$

A synchronized motion of the N particles corresponds to the vehicles moving in the same direction, that is $\theta_k = \theta_j$ for all k, j. A balanced motion of N particles corresponds

to the agents moving in opposite direction.

In order to measure the synchronization and balancing of the particles, we will use the centroid of particle phasors below which is called phase order parameter [25]

$$p_\theta = p(e^{i\boldsymbol{\theta}}) = \frac{1}{N}\sum_{k=1}^{N} e^{i\theta_k}$$

where $\boldsymbol{\theta} = [\theta_1, ..., \theta_N]$. The phase arrangement $\boldsymbol{\theta}$ is called synchronized if the modulus of the phase order parameter equals one, that is $|p_\theta| = 1$ and is called balanced when $|p_\theta| = 0$.

By replacing $u_k = -K\sum_{j=1}^{N}\sin(\theta_j - \theta_k)$ in (2.6), the system (2.6) becomes

$$\begin{aligned} \dot{r}_k &= e^{i\theta_k} \\ \dot{\theta}_k &= -K\sum_{j=1}^{N}\sin(\theta_j - \theta_k). \end{aligned} \tag{2.7}$$

The phase arrangement $p(\theta)$ in (2.7 goes to zero and parallel formation is achieved for $K > 0$. The absolute value of phase arrangement $p(\theta)$ stabilizes at 1 and balanced formation is achieved for $K < 0$.

Circular motion of one particle is achieved when the particle has a constant turning rate ω_0, where $\theta_k(t) = \omega_0 t + \theta_k(0)$, and when its center of motion c_k is fixed, that is $\dot{c_k} = 0$. Similarly, circular formation for N particles is achieved when all the particles have the same turning rate ω_0 and $\dot{c_k} = 0$ with $c_k = c_j$ for all $k, j \in N$.

The center of of rotation c_k for the particle model described in Cartesian coordinates with $c_k = r_k + i\omega_0^{-1}e^{i\theta_k}$ and $\dot{c_k} = e^{i\theta_k} - \omega_0^{-1}u_k e^{i\theta_k}$. for $u_k = \omega_0$, $\dot{c_k} = 0$ and the particle

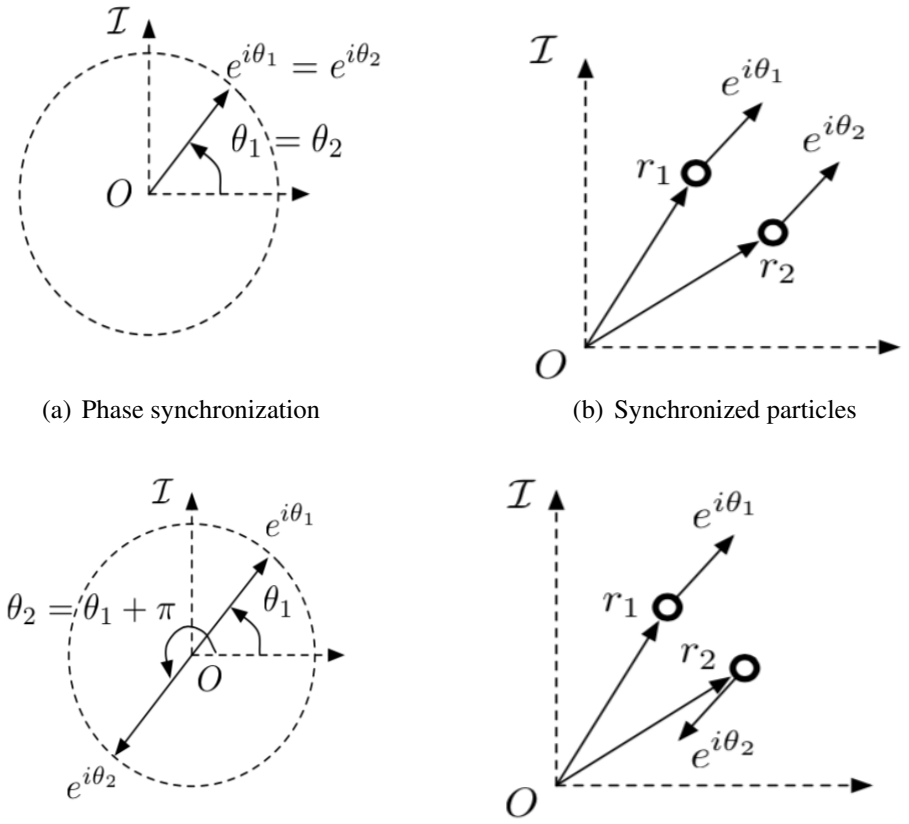

(a) Phase synchronization

(b) Synchronized particles

(c) Phase balancing

(d) Balanced particles

Figure 2.2: Phase synchronization and balancing for $N = 2$. (a,b) two synchronized particles move in parallel; (c,d) two particles with balanced phases move in opposite direction

moves around a fixed circle where $|\omega_0^{-1}|$ is the circle's radius. If $\omega_0 > 0$ the particle moves counterclockwise and it moves clockwise if $\omega_0 < 0$.

Similarly, using the center of rotation described above, the following control law stabilizes the particles around the same circle [25]:

$$u_k = \omega_0(1 + K_0\langle e^{i\theta_k}, L_k\boldsymbol{c}\rangle)$$

with $K_0 > 0$ and where $\langle , \rangle$ is the inner product operator. By replacing u_k in (2.6), the

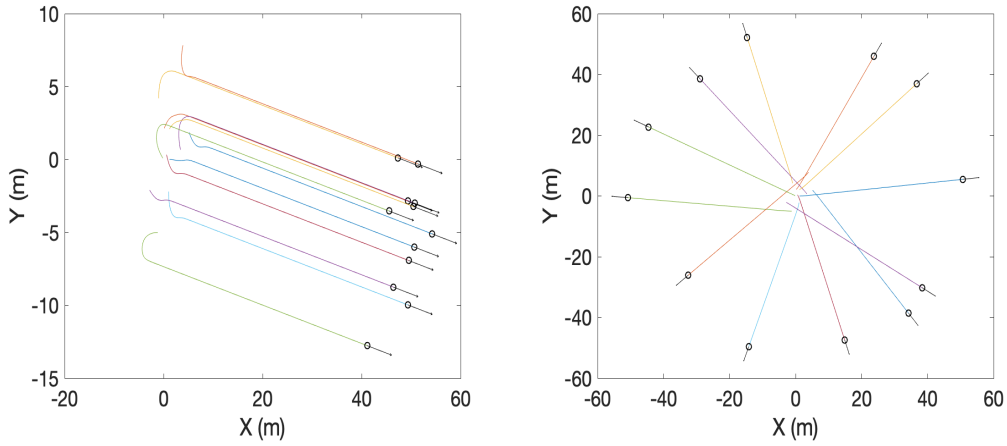

(a) $K < 0$ (b) $K > 0$

Figure 2.3: Simulation of closed loop particle model with all to all phase control (2.7) with $N = 12$. The arrows on each particle represent the phase of each one of them.

system (2.6) becomes:

$$\begin{aligned} \dot{r}_k &= e^{i\theta_k} \\ \dot{\theta}_k &= \omega_0(1 + K_0\langle e^{i\theta_k}, L_k\boldsymbol{c}\rangle). \end{aligned} \tag{2.8}$$

Now consider the case when the velocity of the particles is constant but non-unitary. The particle model becomes:

$$\dot{r}_k = s_k e^{i\theta_k}$$

$$\dot{\theta}_k = u_k,$$

where $r_k \in \mathbb{C}, \theta_k \in \mathbb{T}$, $u_k \in \mathbb{R}$ and $s_k \in \mathbb{R}$ denote the position, phase, steering control and velocity for particle $k \in \mathcal{N}$, respectively.

In order to move a single particle on a circle of radius $|\omega_0^{-1}|$, where $c_k = r_k + i\omega_0^{-1}e^{i\theta_k}$,the position of the center of this circle has to be stabilized on a fixed point. Thus

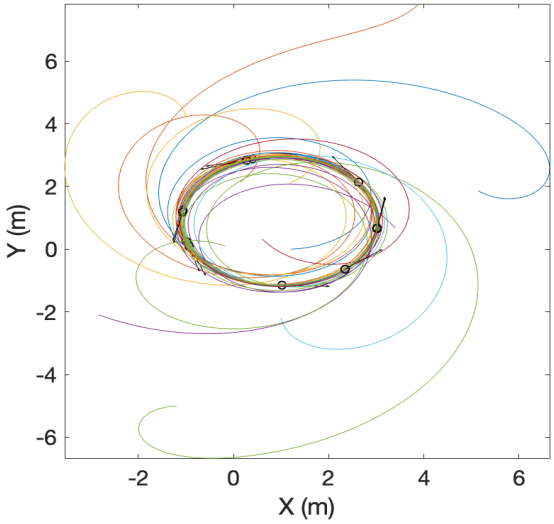

Figure 2.4: Simulation of closed loop particle model with all to all phase control (2.8) with $N = 12$. the arrows on each particle represent the phase of each one of them. all of the particle move around the same circle or radius $\omega_0^{-1} = 2$

we need $\dot{c}_k = 0$ where

$$\dot{c}_k = s_k e^{i\theta_k} - \omega_0^{-1} u_k e^{i\theta_k}$$

By choosing $u_k = \omega_0 s_k$, the particle moves on a fixed circle of radius $|\omega_0^{-1}|$ [37].

Chapter 3: Modeling Swimming Dynamics Using the Chaplygin Sleigh

3.1 Straight Motion

As an example second-order oscillator system with nonlinear dynamics, consider the dynamics and state-feedback control of a single fish robot modeled as a Chaplygin sleigh [33]. The Chaplygin sleigh is a nonholonomic mechanical system that moves in the horizontal plane and is propelled by an internal rotor [34], [33].The nonholonomic constraint is at the trailing edge and is due to the Kutta condition [38], where this constraint permits no velocity in the perpendicular direction of the fish. A rotating reaction wheel at the center of mass of the fish is used to generate translational forward motion [39]

Let $v \in \mathbb{R}$ denote the swimming velocity, $\theta \in \mathbb{S}^1$ the heading angle, and $\omega \in \mathbb{R}$ the angular rate of the fish. The dynamics in state space form are [33]

$$\begin{aligned} \dot{v} &= l\omega^2 - dv \\ \dot{\theta} &= \omega \\ \dot{\omega} &= -\frac{mlv}{b}\omega - \frac{u}{b}\ , \end{aligned} \tag{3.1}$$

where $d \geq 0$ is the drag coefficient, and $m > 0$, $l > 0$, and $b > 0$ are the mass, length,

and moment of inertia, respectively. Choosing the closed-loop control [33]

$$u = b(-K_1\omega - K_2 \sin(\theta_d - \theta)) \ ,$$

where θ_d is the desired heading angle and $K_1, K_2 > 0$ are feedback gains, yields the closed-loop system [33]

$$\begin{aligned} \dot{v} &= l\omega^2 - dv \\ \dot{\theta} &= \omega \\ \dot{\omega} &= -\frac{ml}{b} v\omega + K_1\omega + K_2 \sin(\theta_d - \theta) \end{aligned} \tag{3.2}$$

The system (3.2) can be divided into a slow and fast subsystems [33]. The fast v subsystem can be written as

$$\dot{v} = d\left(\frac{l}{d}\omega^2 - v\right) \ . \tag{3.3}$$

For d sufficiently large, this subsystem converges to $v = \frac{l}{d}\omega^2$. Let $a = \frac{ml^2}{bd} > 0$. With the substitution $v = \frac{l}{d}\omega^2$, the slow (θ, ω) subsystem becomes [33]

$$\begin{aligned} \dot{\theta} &= \omega \\ \dot{\omega} &= -a\omega^3 + K_1\omega + K_2 \sin(\theta_d - \theta) \end{aligned} \tag{3.4}$$

Observe that (3.4) gives the equations of motion of a pendulum with nonlinear damping and natural frequency $\sqrt{K_2}$ [33]. The system (3.4) has two equilibrium points $(\theta, \omega) = (\theta_d, 0)$ and $(\theta, \omega) = (\pm\pi - \theta_d, 0)$ (with sign depending on θ_d). Both equilibria are unstable and the system exhibits a stable limit cycle centered on $(\theta_d, 0)$ in the (θ, ω)

Parameter	Symbol	Value
Mass	m	1.4 kg
Length	l	0.31 m
Drag coefficient	d	0.5
Moment of inertia	b	0.1395 kg·m^2
Desired heading	θ_d	0.78 rad
Control gains	(K_1, K_2)	$(0.5, 2)$

Table 3.1: Parameters used to simulate the closed-loop fish-robot system (3.2)

plane [33]. The corresponding limit cycle of the full system (3.2) lies in the (v, ω) plane. is centered on $(K_1 b/(ml), 0)$ [33]. The limit cycle propels the fish robot in the desired direction by flapping the tail. Simulation of the closed loop control using the parameters provided in Table (3.1), where these parameters originate from the original fish design [33], are shown in Figure (3.1)below.

3.1.1 Bifurcation Analysis of Closed-loop System

The closed-loop system exhibits bifurcation behavior in which the desired limit cycle corresponding to forward swimming behavior is achieved only for certain values of the control gains K_1 and K_2 [33]. The average swimming velocity is proportional to K_1, but if K_1 is too large, the angular rate in the resulting limit cycle does not switch signs and the model fish spins in a circle [33]. We now establish the existence of the desired limit cycle and determine the allowable range of gains.

Without loss of generality, let the reference angle be $\theta_d = 0$. Substituting θ_d in (3.4), the system (3.4) becomes:

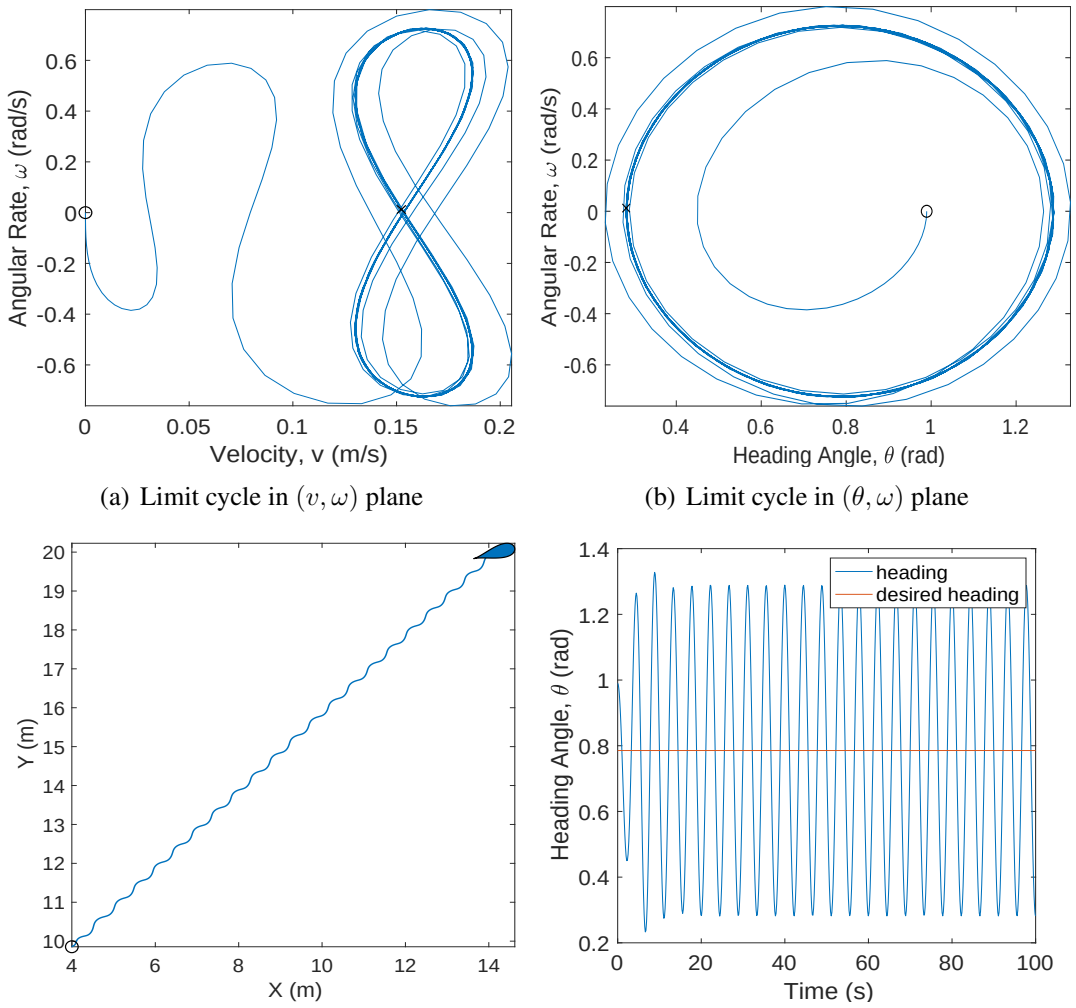

(a) Limit cycle in (v, ω) plane

(b) Limit cycle in (θ, ω) plane

(c) Paths in the (x, y) plane

(d) Heading angle time history

Figure 3.1: Simulation of a single fish showing the robot tracking a constant heading

$$\begin{aligned} \dot{\theta} &= \omega \\ \dot{\omega} &= -a\omega^3 + K_1\omega - K_2 \sin\theta, \end{aligned} \tag{3.5}$$

The Jacobian of (3.5) with respect to $z = (\theta, \omega)$ is

$$\frac{\partial f}{\partial z} = \begin{bmatrix} 0 & 1 \\ -K_2 \cos\theta & -3a\omega^2 + K_1 \end{bmatrix}.$$

which implies the origin $(0, 0)$ is an unstable node or focus and the point $(\pm\pi, 0)$ is a saddle. To facilitate analysis of the limit cycle in (3.5), let $K_1 = a$, which yields

$$\dot{\theta} = \omega \tag{3.6}$$

$$\dot{\omega} = a(-\omega^3 + \omega) - K_2 \sin\theta. \tag{3.7}$$

The linearization of (3.6)–(3.7) at $(\theta, \omega) = (0, 0)$ becomes

$$\left.\frac{\partial f}{\partial z}\right|_{(0,0)} = \begin{bmatrix} 0 & 1 \\ -K_2 & a \end{bmatrix},$$

which has eigenvalues $\lambda_{1,2} = \frac{a}{2} \pm \frac{1}{2}\sqrt{a^2 - 4K_2}$. Therefore, the eigenvalues are complex if $|a| < 2\sqrt{K_2}$. Consider a as a bifurcation parameter. For $-2\sqrt{K_2} < a < 0$, the origin is a stable focus and, for $0 < a < 2\sqrt{K_2}$, the origin is an unstable focus. Therefore, as a passes through zero, There is a Hopf bifurcation giving rise to a stable limit cycle for $0 < a < 2\sqrt{K_2}$ (and an unstable limit cycle for $-2\sqrt{K_2} < a < 0$).

3.2 Circular Motion

In the case of straight motion, the desired heading angle θ_d was constant, and the fish was propelled forward in the direction of the desired angle while keeping the flapping motion of the tail due to the angular velocity switching sign back and forth in the limit cycle. Now in order to drive a single around a circle, I let the fish track a time varying heading angle of the form $\theta_d = \omega_d t + \theta_k(0)$ and replace $\theta_d = 0$ by $\theta_d = \omega_d t + \theta_k(0)$ in (3.4).

Consider the system (3.4) and let $\gamma = \theta - \theta_d$ and $\dot{\gamma} = \omega - \omega_d$. By changing the coordinates from (ω, θ) to (ω, γ) the system (3.4) becomes:

$$\begin{aligned} \dot{\gamma} &= \omega - \omega_d \\ \dot{\omega} &= -a\omega^3 + K_1\omega - K_2 \sin(\gamma) \end{aligned} \tag{3.8}$$

Proposition 2. *The closed loop form (3.8) moves the Chaplygin sleigh on a circle on average.*

Proof. I choose the Lyapunov candidate:

$$V = \frac{1}{2}\omega^2 + K_2[1 - \cos(\gamma)].$$

By taking the derivative of V along the system (3.8)

$$\begin{aligned}\dot{V} &= \dot{\omega}\omega + (\omega - \omega_d)\sin(\gamma) \\ &= -a\omega^4 + K_1\omega^2 - K_2\omega\sin(\gamma) + K_2\omega\sin(\gamma) - K_2\omega_d\sin(\gamma) \\ &= -a\omega^4 + K_1\omega^2 - K_2\omega_d\sin(\gamma) \\ &\leq -a\omega^4 + K_1\omega^2 + K_2|\omega_d|.\end{aligned} \tag{3.9}$$

From this Lyapunov analysis, I can conclude the the solutions are trapped in an invariant set. This set can be found by the following polynomial:

$$-a\omega^4 + K_1\omega^2 + K_2|\omega_d| = 0. \tag{3.10}$$

using change of variables, $x = \omega^2$ to obtain

$$ax^2 - K_1x - K_2|\omega_d| = 0. \tag{3.11}$$

The solutions polynomial (3.11) are x_1 and x_2 where

$$x_{1,2} = \frac{K_1 \pm \sqrt{K_1^2 + 4a|\omega_d|}}{2a}.$$

Since $x > 0 \implies x = \omega^2 = \frac{K_1+\sqrt{K_1^2+4a|\omega_d|}}{2a}$ is the only valid solution to (3.11). Therefore, $\omega = \pm\sqrt{\frac{K_1+\sqrt{K_1^2+4a|\omega_d|}}{2a}}$ is the only solution to (3.10) and when $\|\omega\| > \sqrt{\frac{K_1+\sqrt{K_1^2+4a|\omega_d|}}{2a}}$, the time derivative $\dot{V} \leq 0$. Also, for $\|\omega\| = \sqrt{\frac{K_1+\sqrt{K_1^2+4a|\omega_d|}}{2a}}$,(3.9)

gives $\dot{V} = 0$, therefore the set $\Omega = \{|\omega| < \sqrt{\frac{K_1+\sqrt{K_1^2+4a|\omega_d|}}{2a}}\}$ is positively invariant and solutions of (3.8) are trapped in Ω.

Next, equilibrium points of (3.8) are derived, where $(\dot{\gamma}, \dot{\omega}) = (0, 0)$. Setting $\dot{\gamma} = 0$ in (3.8), it is clear that $\omega = \omega_d$ at the equilibrium. Furthermore, $\dot{\omega} = 0$ requires $\gamma = \arcsin\left(\frac{-a\omega_d^3+K_1\omega_d}{K_2}\right)$

Thus, $(\gamma, \omega) = (\arcsin\left(\frac{-a\omega_d^3+K_1\omega_d}{K_2}\right), \omega_d)$ is an equilibrium point of (3.8). In order for this equilibrium point to exist, the following inequality must be satisfied:

$$-1 \leq \frac{a\omega_d^3 - K_1\omega_d}{K_2}) \leq 1$$

Linearizing (3.8) around the equilibrium point $z = (\gamma, \omega) = (\arcsin\left(\frac{-a\omega_d^3+K_1\omega_d}{K_2}\right), \omega_d)$ yields the following linearized matrix

$$\frac{\partial f}{\partial z} = \begin{bmatrix} 0 & 1 \\ -K_2\cos\gamma & -3a\omega^2 + K_1 \end{bmatrix}$$

$$\frac{\partial f}{\partial z} = \begin{bmatrix} 0 & 1 \\ -K_2\cos\left[\arcsin\left(\frac{-a\omega_d^3+K_1\omega_d}{K_2}\right)\right] & -3a\omega_d^2 + K_1 \end{bmatrix}$$

This system has the two following eigenvalues

$$\lambda_{12} = -3a\omega_d^2 + K_1 \pm \sqrt{(-3a\omega_d^2 + K_1)^2 - 4K_2\cos\left[\arcsin\left(\frac{-a\omega_d^3 + K_1\omega_d}{K_2}\right)\right]}.$$

The desired behavior that we want for the fish is a closed limit cycle around ω_d. In

order to achieve that, the equilibrium point where $\omega = \omega_d$ must exist first of all, and the eigenvalues of the equilibrium point must have positive real parts and a complex part so the equilibrium would be an unstable focus. These conditions are met when:

$$-1 \leq \frac{a\omega_d^3 - K_1\omega_d}{K_2} \leq 1, \tag{3.12}$$

$$K_1 \geq 3a\omega_d^2, \tag{3.13}$$

and

$$-3a\omega_d^2 + K_1 \leq 2\sqrt{K_2 \cos\left[\arcsin\left(\frac{-a\omega_d^3 + K_1\omega_d}{K_2}\right)\right]}. \tag{3.14}$$

When these conditions are met, the equilibrium point is an unstable focus and we have a periodic orbit around ω_d. and the fish moves around a circle on average which completes the proof.

□

Nevertheless, the angular velocity ω should not always have the same sign, it should go from positive and negative periodically. To achieve this, while satisfying the above requirement, ω_d is chosen to be small enough so that ω oscillates from negative to positive and vice versa.

In order to illustrate proposition 2, and since(3.8) is an approximate system only,

Parameter	Symbol	Value
Mass	m	1.4 kg
Length	l	0.31 m
Drag coefficient	d	0.5
Moment of inertia	b	0.1395 kg·m^2
Desired heading	θ_d	$\omega_d t + 0.78$ rad
Desired angular velocity	ω_d	0.2 rad/s
Control gains	(K_1, K_2)	$(0.5, 2)$

Table 3.2: Parameters used to simulate the closed-loop fish-robot system (3.2) while meeting all requirements

the fish is simulated using the closed loop form below:

$$\begin{aligned} \dot{v} &= l\omega^2 - dv \\ \dot{\gamma} &= \omega - \omega_d \\ \dot{\omega} &= -\frac{ml}{b} v\omega + K_1\omega - K_2 \sin(\gamma) \end{aligned} \tag{3.15}$$

where the simulation parameters are listed in (3.2)

By choosing $K_1 = 0.5, K_2 = 2$ and $\omega_d = 0.2 rad/s$ conditions (3.12),(3.13) and (3.14) are met. Simulation results of system (3.15) are represented in figure (3.2-a)

In (3.2-a) and (3.2-b), the limit cycle orbits ω_d and the values of ω oscillate around ω_d from positive to negative periodically. Therefore we can see the fish tail flapping back and forth which is clear from the trajectory path in (c). Also, as is seen in (d), the trajectory tracks θ_d perfectly.

In figure (3.2), the fish moves over an average radius $|\omega_0^{-1}|$ and that the average value of the center of motion is fixed. the average value of the centre of motion of the fish

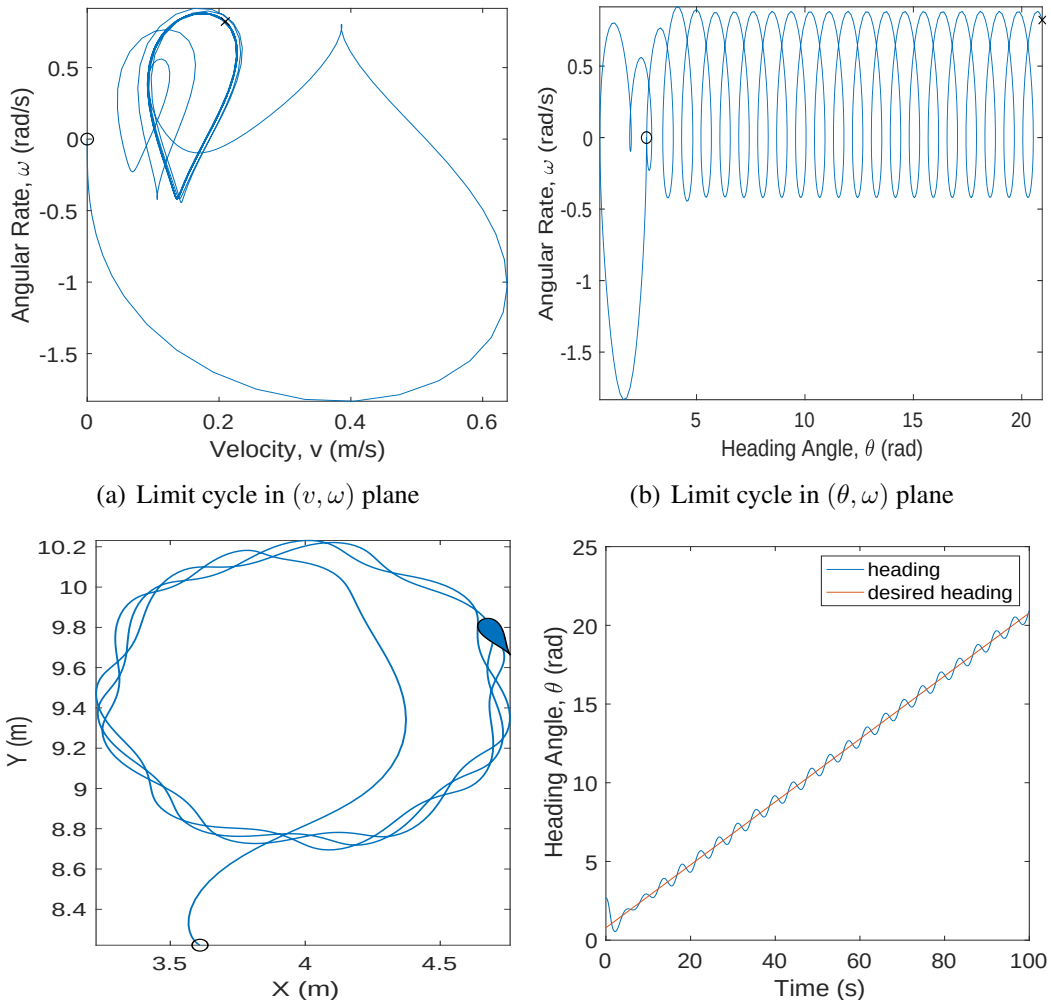

(a) Limit cycle in (v, ω) plane

(b) Limit cycle in (θ, ω) plane

(c) Paths in the (x, y) plane

(d) Heading angle time history

Figure 3.2: Simulation of a single fish showing the robot tracking the desired circular trajectory while maintaining tail flapping

is analyzed next, which is its value at the equilibrium point $(\gamma, \omega) = (\arcsin\left(\frac{-a\omega_d^3 + K_1\omega_d}{K_2}\right), \omega_d)$.

$$\begin{aligned} \overline{c_k} &= \overline{r_k} + i\omega_0^{-1}\overline{e^{i\theta_k}} \\ \overline{c_k} &= \overline{r_k} + i\omega_0^{-1}e^{i\theta_d} \\ \overline{\dot{c}_k} &= \overline{s_k}e^{i\theta_d} - \omega_0^{-1}\omega_d e^{i\theta_d} \end{aligned} \tag{3.16}$$

the average value of the centre of motion is fixed when:

$$\begin{aligned} \overline{\dot{c}_k} &= 0 \\ \overline{\dot{c}_k} = 0 &\implies \overline{s_k} = \omega_0^{-1}\omega_d \end{aligned} \tag{3.17}$$

Since the average value of s_k is $\overline{s_k} = \frac{bk_1}{ml}$ [33], then

$$\omega_d = \frac{\overline{s_k}}{\omega_0^{-1}} = \frac{\frac{bk_1}{ml}}{\omega_0^{-1}}. \tag{3.18}$$

moves the fish around a stable circle of radius

$$|\omega_0^{-1}| = |\frac{\frac{bk_1}{ml}}{\omega_d}|. \tag{3.19}$$

Now in the other case when we chose $K_1 = 1, K_2 = 1$ and $\omega_d = 5$, the condition (3.12) is not met. In this case, the equilibrium point does not exist. To verify this, the system (3.15) is simulated using parameters provided in Table (3.2) with $\omega_d = 5rad/s$ and $K_2 = 1$. Simulation results are represented in Figure (3.2).

The angular rate ω orbits the boundary of the set $\Omega = \{\|\omega\| < \sqrt{\frac{K_1+\sqrt{K_1^2+4a|\omega_d|}}{2a}}\}$ as shown in Fig.3.2b but does not oscillate from positive to negative periodically. Hence, the tail of the fish does not flap as shown in Fig.3.2c, therefore there is no propulsion force and the fish does not swim.The trajectory shown in Fig.3.2c could be achieved only if there is propulsion force, which is not the case here since the tail does not flap because the reaction wheel does not oscillate from positive to negative periodically.In this case, the fish spins on a circle centered around the fish's centre of mass. In addition, the heading angle does not track the desired heading angle θ_d, as shown in Fig.3.2d, since the

equilibrium point does not exist.

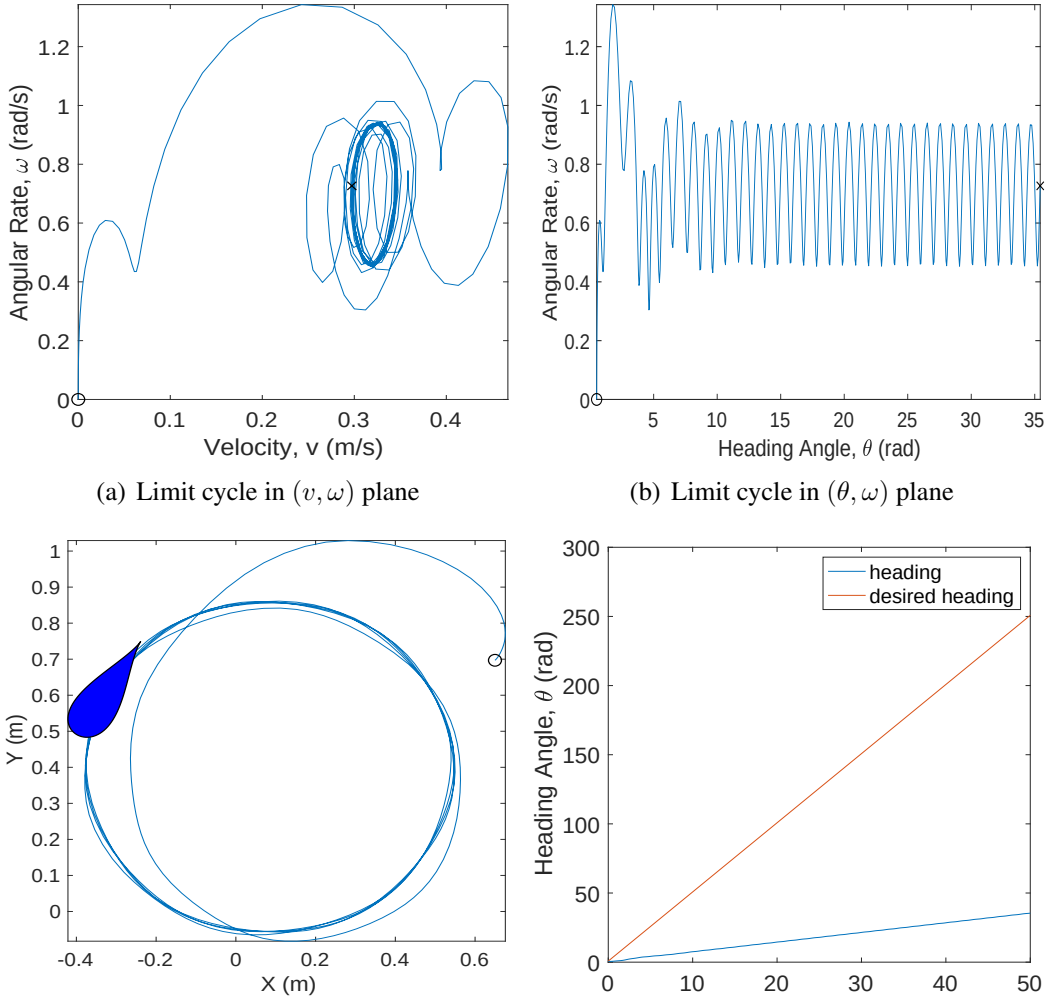

(a) Limit cycle in (v, ω) plane

(b) Limit cycle in (θ, ω) plane

(c) Paths in the (x, y) plane

(d) Heading angle time history

Figure 3.3: Simulation of a single fish when no equilibrium point exists showing the robot not able to track the desired trajectory.

Chapter 4: Synchronized Swimming Via Angular Velocity Consensus

4.1 Synchronization of Second-order Oscillators

Consider a collection of N identical oscillating agents whose orientations live on $\mathbb{T}^N$ with dynamics given by (2.2) and (2.3). Furthermore, without loss of generality, suppose the control $u_k(\boldsymbol{\theta}, \boldsymbol{\omega}) = \bar{u}_k(\theta_k, \omega_k) + \nu_k(\boldsymbol{\omega})$, where

$$\bar{u}_k = K_1 g(\omega_k) - K_2 \sin(\theta_k - \theta_d) \tag{4.1}$$

$$\nu_k = -K_3 L_k \boldsymbol{\omega}, \tag{4.2}$$

K_1, K_2 and $K_3 > 0$, and L_k is the kth row of the Laplacian matrix (2.1) of a connected undirected graph G representing the interaction topology of the agents. The term $L_k\boldsymbol{\omega} = \sum_{j \neq k}(\omega_k - \omega_j)$ is the sum of the angular rate of the kth agent relative to the angular rate of all connected agents. Substituting the control $u_k(\boldsymbol{\theta}, \boldsymbol{\omega}) = \bar{u}_k(\theta_k, \omega_k) + \nu_k(\boldsymbol{\omega})$ with (4.1) and (4.2) into (2.2) and (2.3) gives

$$\dot{\theta}_k = \omega_k \tag{4.3}$$

$$\dot{\omega}_k = f(\omega_k) - K_2 \sin(\theta_k - \theta_d) - K_3 L_k \boldsymbol{\omega}\ , \tag{4.4}$$

Proposition 3. *The second-order oscillator system* (4.3), (4.4) *with network topology given by the Laplacian matrix* L *of a connected interaction graph* $G = (\mathcal{N}, E)$*, reaches consensus* (2.4), (2.5) *on the tangent bundle of the* N*-torus if (i)* $K_3 \gg K_1, K_2$ *and (ii) if* $f(\omega_k) = f(\omega_j)$ *for all* $k, j \in N$

Proof. (4.4) is of the following form:

$$\dot{\omega}_k = f(\omega_k) - K_2 \sin(\theta_k - \theta_d) - K_3 L_k \boldsymbol{\omega},$$

by dividing (4.4) by K_3 I get:

$$\frac{1}{K_3}\dot{\omega}_k = \frac{1}{K_3} f(\omega_k) - \frac{K_2}{K_3} \sin(\theta_k - \theta_d) - L_k \boldsymbol{\omega},$$

Let $\boldsymbol{z} = L\boldsymbol{\omega}$, for $K_3 \gg K_1, K2$ I have:

$$\epsilon\dot{\omega}_k = -\epsilon f(\omega_k) - \epsilon \sin(\theta_k - \theta_d) - z_k.$$

where $\epsilon = \frac{1}{K_3} \approx \frac{K_2}{K_3}$.

Consider the updated state space form

$$\begin{aligned} \dot{\boldsymbol{\theta}} &= \boldsymbol{\omega} \\ \dot{\boldsymbol{\omega}} &= g(\boldsymbol{\omega}) - K_2 \sin(\boldsymbol{\theta} - \boldsymbol{\theta_d}) - K_3 \boldsymbol{z} \\ \dot{\boldsymbol{z}} &= L\dot{\boldsymbol{\omega}} = L[f(\boldsymbol{\omega}, \boldsymbol{\theta}) - K_2 \sin(\boldsymbol{\theta} - \boldsymbol{\theta_d}) - K_3 \boldsymbol{z}], \end{aligned} \tag{4.5}$$

for $K_3 \gg 1$, I have $\epsilon\dot{\boldsymbol{z}} = \epsilon L\dot{\boldsymbol{\omega}}$.

$$\epsilon\dot{\boldsymbol{z}} = \begin{bmatrix} \epsilon(N-1)\dot{\omega_1} - \epsilon\dot{\omega_2} \cdots - \epsilon\dot{\omega_n} \\ \epsilon(N-1)\dot{\omega_2} - \epsilon\dot{\omega_1} \cdots - \epsilon\dot{\omega_n} \\ \vdots \\ \epsilon(N-1)\dot{\omega_n} - \epsilon\dot{\omega_1} \cdots - \epsilon\dot{\omega_{n-1}} \end{bmatrix}$$

$$\epsilon\dot{\boldsymbol{z}} = \begin{bmatrix} \epsilon\Phi_1(\boldsymbol{\omega}, \boldsymbol{\theta}) - \frac{1}{N} z_1 \\ \vdots \\ \epsilon\Phi_n(\boldsymbol{\omega}, \boldsymbol{\theta}) - \frac{1}{N} z_n \end{bmatrix}$$

where $\boldsymbol{\Phi}(\boldsymbol{\omega}, \boldsymbol{\theta})$ is a nonlinear term. Therefore system (4.5) becomes:

$$\begin{aligned} \dot{\boldsymbol{\theta}} &= \boldsymbol{\omega} \\ \dot{\boldsymbol{\omega}} &= f(\boldsymbol{\omega}) - K_2 \sin(\boldsymbol{\theta} - \boldsymbol{\theta_d}) - K_3 \boldsymbol{z} \\ \epsilon\dot{\boldsymbol{z}} &= \epsilon\boldsymbol{\Phi}(\boldsymbol{\omega}, \boldsymbol{\theta}) - \frac{1}{N}\boldsymbol{z}. \end{aligned} \tag{4.6}$$

For $\epsilon = 0$ I have $\boldsymbol{z} = h(x) = 0$ and I write $\dot{z} = g(t, z, \epsilon)$.By taking $y = z - h(x) = z$ and $\frac{\partial \boldsymbol{y}}{\partial \tau} = \epsilon\dot{z} = g(t, z, 0)$ where $\tau = \frac{t}{\epsilon}$. The problem is then reduced to a boundary layer problem [40] where:

$$\dot{\boldsymbol{y}} = -\frac{1}{N}\boldsymbol{y}.$$

By replacing $z = 0$ into the system (4.6) becomes:

$$\begin{aligned} \dot{\boldsymbol{\theta}} &= \boldsymbol{\omega} \\ \dot{\boldsymbol{\omega}} &= f(\boldsymbol{\omega}) - K_2 \sin(\boldsymbol{\theta} - \theta_d). \end{aligned} \tag{4.7}$$

where (4.7) is the slow subsystem.

$$\dot{\boldsymbol{y}} = -\frac{1}{N}\boldsymbol{y}. \tag{4.8}$$

and (4.8) is the fast subsystem.

Equation(4.8) is clearly asymptotically stable, hence the angular velocities reach consensus.

Therefore, $\omega_k \equiv \omega_j$, which implies $\dot{\omega}_k = \dot{\omega}_j$ and $f_k = f_j$. Therefore, (4.7) implies $\sin(\theta_k - \theta_d) = \sin(\theta_j - \theta_d)$, which is true if $\theta_k = \theta_j$ or $\pi - \theta_j$. The second solution is a contradiction, because $\dot{\theta}_k \neq -\dot{\theta}_j$.Therefore the heading angle is synchronized for all the vehicles.

□

4.2 Synchronized Swimming: Straight Motion

Consider a collection of N robotic fish, indexed by $k = 1, \cdots, N$, with Chaplygin-sleigh dynamics (3.1). The closed-loop system (3.4) is augmented with consensus control to become

$$\begin{aligned} \dot{\theta}_k &= \omega_k \\ \dot{\omega}_k &= -a\omega_k^3 + K_1\omega_k + K_2\sin(\theta_d - \theta_k) - K_3 L_k \boldsymbol{\omega} \end{aligned} \tag{4.9}$$

The following Corollary applies Proposition 3 to the robotic fish system (4.9).

Corollary 4. *The system (4.9) reaches consensus* (2.4), (2.5) *on the tangent bundle of the*

N-torus.

Proof. Let $g(\omega_k) = -a\omega_k^3$ and $f_k = g(\omega_k) + K_1\omega_k = -a\omega_k^3 + K_1\omega_k$ so that (4.5) is in the form of (4.3) and (4.4). Note that $f_k = f_j$ for all $k, j \in N$.Then by letting $K3 \gg K_2, K_1$ Proposition 3 is satisfied, which completes the proof.

□

Remark 5. *Since the system (4.9) reduces to (4.7) which is the same as (3.4), hence each fish maintains the same behavior as in (3.4), and each fish have an identical unstable equilibrium point which is* $(\omega, \theta) = (0, \theta_d)$. *Therefore, the consensus control in Corollary 4 drives the heading of the agents to oscillate around the desired heading angle* θ_d *too.*

Corollary 4 is illustrated by simulating the closed-loop Chaplygin sleigh fish robot system with the parameters listed in Table 3.1,with $K_1 = 0.5, K_2 = 2$, $K_3 = 6$ and with $N = 8$ fish initialized with random headings in the range $[0, \pi]$ and zero velocity and angular rate. Although Corollary 4 applies to the approximate Chaplygin sleigh dynamics (3.4), we simulate the full dynamics (3.1) with the consensus control law (4.1), (4.2). Fig. 4.2 shows all N fish converge to the same limit cycle in the (v, ω) plane. Similarly, the fish school converges to a limit cycle in the (θ, ω) plane that is centered around the desired heading angle $\theta_d = 0.78$ rad Fig. 4.2b. (The symbols o and x in Figs. 4.2a and 4.2b indicate the initial and final states of the system at the beginning and end, respectively, of the simulation.) The overlapping x markers in Figs. 4.2a and 4.2b indicate that the heading, angular rate, and velocity of the fish reach consensus. The initial positions of the fish were initialized randomly near the origin and the resulting motion of the robot fish

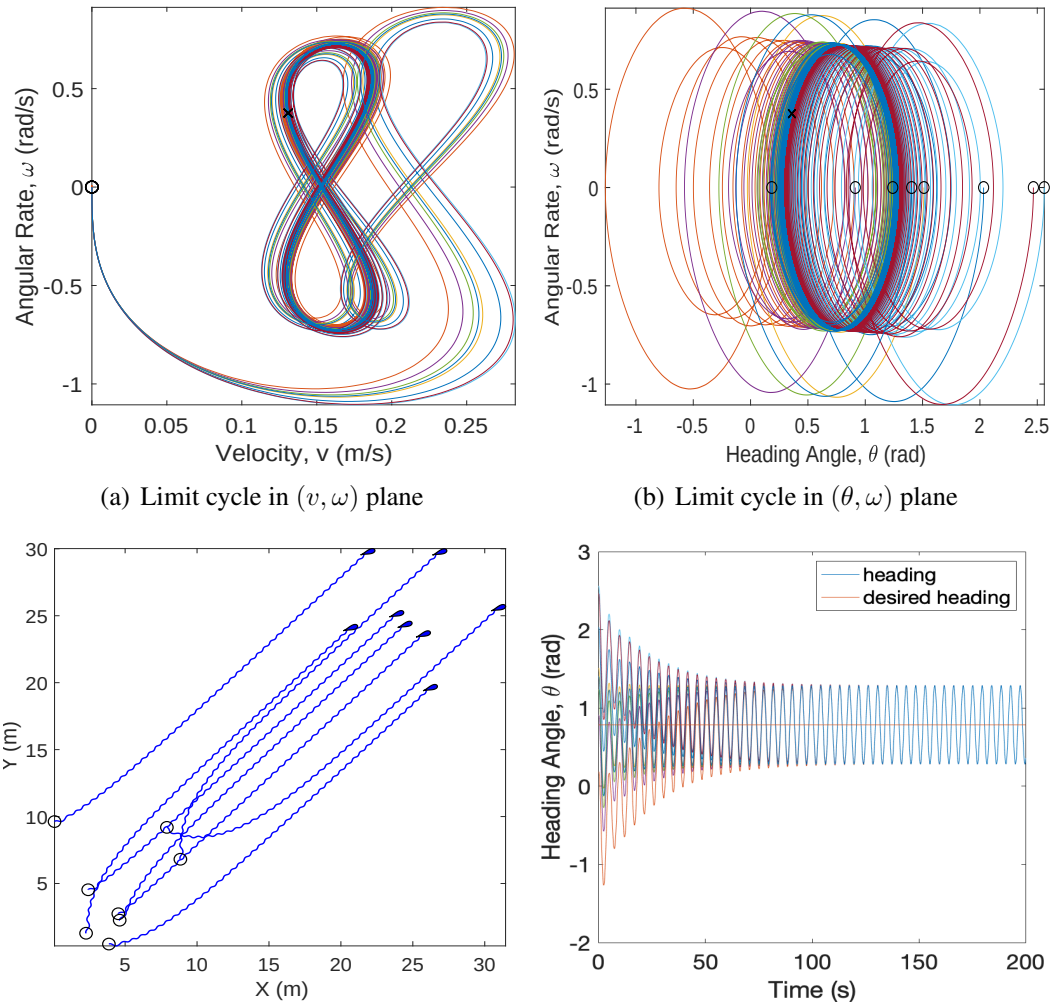

(a) Limit cycle in (v, ω) plane

(b) Limit cycle in (θ, ω) plane

(c) Paths in the (x, y) plane

(d) Heading angle time history

Figure 4.1: Simulation of $N = 8$ Chaplygin sleigh fish robots reaching consensus. (c)The black o and x markers in Figs.(a),(b) and indicates the initial and final simulation states, respectively, of the multi-agent system.)

center of mass in the (x, y) plane shows that they swim with synchronized heading and flapping (angular rate) with an average heading of 45 degrees 4.2c. Fig. 4.2d illustrates the heading synchronization over time about the desired heading angle indicated by a solid horizontal line.

4.3 Synchronized Swimming: Circular Motion

Now in order to drive all of the fish around different circles while synchronizing tail flapping, I let each fish track a time varying heading angle of the form $\theta_d = \omega_d t + \theta_k(0)$. Therefore the value of θ_d in (4.5) is updated to the the new value that drives a single fish in circle, as in section 3.2

Simulation results are represented in Fig.(4.3) using the parameters presented in Table (3.2) with $\omega_d = 0.2rad/s, K_1 = 0.5, K_2 = 2$ and $K_3 = 6$. same consensus is reached is an Fig.(4.2) with the only difference that the fish move in circle while also keeping their flapping characteristics.

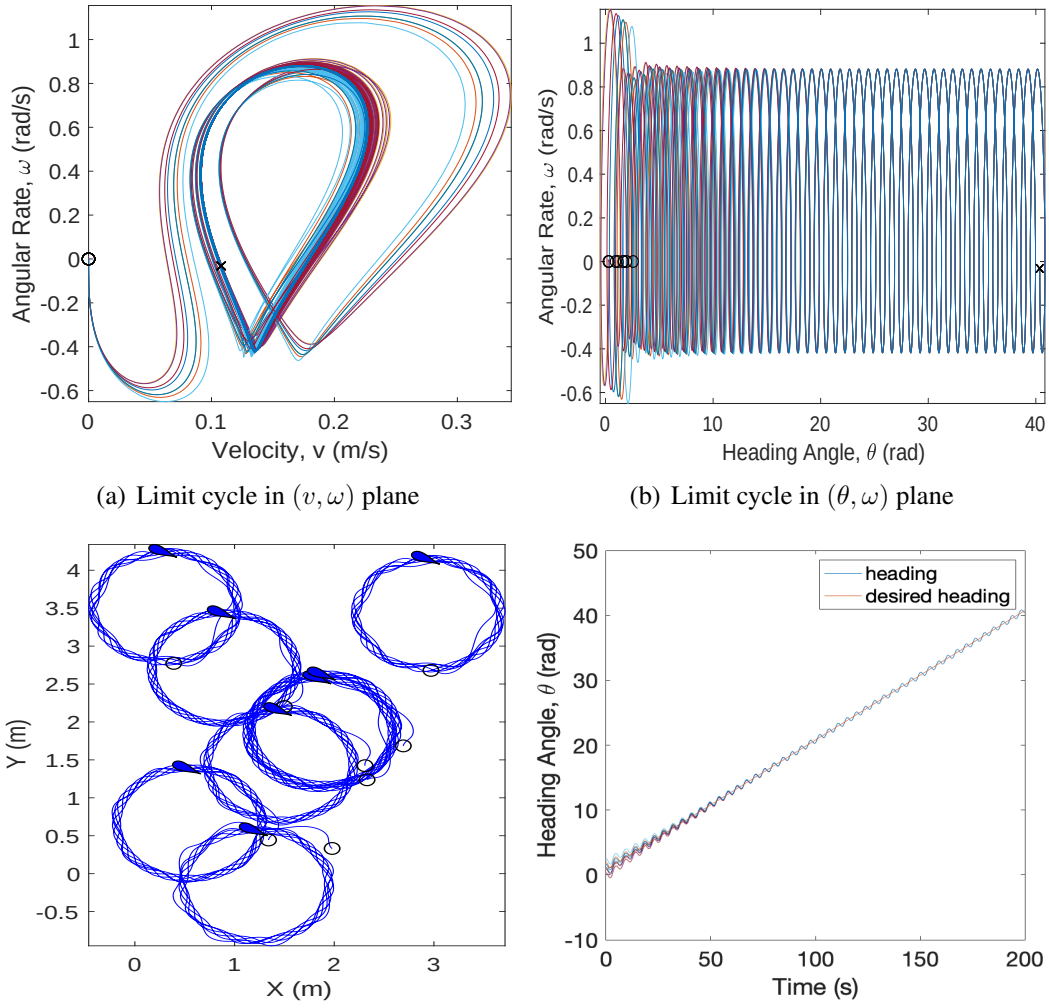

(a) Limit cycle in (v, ω) plane

(b) Limit cycle in (θ, ω) plane

(c) Paths in the (x, y) plane

(d) Heading angle time history

Figure 4.2: Simulation of $N = 8$ Chaplygin sleigh fish robots reaching consensus while moving in circles.

Chapter 5: Formation Control With Phase Angle Coupling

As mentioned before, parallel and circular formation have been achieved before on first and second order self propelled particles. These models are very primitive and don't take into account vehicle dynamics and motion requirements. In this section the previous model of self propelled particles is extended to the Chaplygin sleigh fish. I therefore achieve parallel and circular motion of multiple fish while maintaining fish tail flapping. knowledge of relative orientation is assumed in parallel formation in addition to relative position of the centre of motion later in circular formation.

5.1 Parallel Formation Control

Consider a collective of N Chaplygin sleighs, each sleigh is labeled with an index k or j from the set $\mathcal{N} \triangleq \{1, \ldots, N\}$. by choosing

$$u_k = -bK_1\omega_k - bK_2 \sum_{j=1}^{N} \sin(\theta_j - \theta_k)$$

the system (3.1) becomes:

$$\begin{aligned}
\dot{v}_k &= l\omega_k^2 - dv_k \\
\dot{\theta}_k &= \omega_k \\
\dot{\omega}_k &= -\frac{mlv_k}{b}\omega_k + K_1\omega_k + K_2\sum_{j=1}^{N}\sin(\theta_j - \theta_k)
\end{aligned} \tag{5.1}$$

The system (5.1) can be divided into a slow and fast subsystems. The v subsystem can be written as

$$\dot{v}_k = d\left(\frac{l}{d}\omega_k^2 - v_k\right)$$

For d sufficiently large, the subsystem (2) converges to $v_k = \frac{l}{d}\omega_k^2$. Using $a = \frac{ml^2}{bd} > 0$, I get:

$$\begin{aligned}
\dot{\theta}_k &= \omega_k \\
\dot{\omega}_k &= -a\omega_k^3 + K_1\omega_k + K_2\sum_{j=1}^{N}\sin(\theta_j - \theta_k)
\end{aligned} \tag{5.2}$$

Proposition 6. *Under the closed loop control form (5.2), the fishes move in parallel for arbitrary number N of fish.*

Proof. :

Let:

$$\boldsymbol{U(\theta)} = \frac{1}{2N} \mid \sum_{j=1}^{N} e^{i\theta_j} \mid^2 .$$

Then

$$\frac{\partial U}{\partial \theta_k} = \frac{1}{N}\sum_{j=1}^{N}\sin(\theta_j - \theta_k).$$

And

$$\dot{U} = \sum_{k=1}^{N} \frac{\partial U}{\partial \theta_k} \frac{\partial \theta_k}{\partial t}$$

$$\dot{U} = \frac{1}{N} \sum_{k=1}^{N} \omega_k \sum_{j=1}^{N} \sin(\theta_j - \theta_k).$$

Now let

$$V = \frac{1}{2} \boldsymbol{\omega^t \omega} - K_2 N \boldsymbol{U(\theta)}$$

By taking the lyapunov derivative with respect to (5.2) I get the following equality:

$$\begin{aligned}
\dot{V} &= \boldsymbol{\dot{\omega}^T \omega} - K_2 N \boldsymbol{\dot{U}} \\
&= \sum_{k=1}^{N} \left(-a\omega_k^4 + K_1 \omega_k^2 + K_2 \omega_k \sum_{j=1}^{N} \sin(\theta_j - \theta_k) \right) - K_2 N \boldsymbol{\dot{U}} \\
&= \sum_{k=1}^{N} \left(-a\omega_k^4 + K_1 \omega_k^2 + K_2 \omega_k \sum_{j=1}^{N} \sin(\theta_j - \theta_k) \right) - K_2 \sum_{k=1}^{N} \omega_k \sum_{j=1}^{N} \sin(\theta_j - \theta_k) \\
&= \sum_{k=1}^{N} \left(-a\omega_k^4 + K_1 \omega_k^2 \right) + K_2 \sum_{k=1}^{N} \omega_k \sum_{j=1}^{N} \sin(\theta_j - \theta_k) - K_2 \sum_{k=1}^{N} \omega_k \sum_{j=1}^{N} \sin(\theta_j - \theta_k) \\
&= \sum_{k=1}^{N} (-a\omega_k^4 + K_1 \omega_k^2)
\end{aligned} \tag{5.3}$$

Since $\dot{V} < 0$ for $\omega_k \notin \Omega$ and $\dot{V} > 0$ for $\omega_k \in \Omega$ where $\Omega = \{\|\omega_k\| \leq \sqrt{\frac{K_1}{a}}\}$ then the set Ω is positively invariant and all of the solutions are trapped in Ω

In order to complete the proof, I consider the case of $N = 2$ vehicles then generalize for arbitrary N.

The equilibrium points of (5.2) for $N = 2$ are:

$$z_1 = (\omega_1, \omega_2, \theta_1, \theta_2) = (0, 0, \theta_0, \theta_0)$$

$$z_2 = (\omega_1, \omega_2, \theta_1, \theta_2) = (0, 0, \theta_0, \theta_0 + \pi)$$

$$z_3 = (\omega_1, \omega_2, \theta_1, \theta_2) = (0, 0, \theta_0 + \pi, \theta_0)$$

The equilibrium point z_1 corresponds to the parallel formation. now in order to make the system (5.1) oscillate around this equilibrium point, it needs to be an unstable focus. To establish this we analyze The jacobian A of the system (4.7) around the equilibrium point z_1 is:

$$A = \frac{\partial f}{\partial z} = \begin{bmatrix} 0 & 0 & 1 & 0 \\ 0 & 0 & 0 & 1 \\ -K_2\cos(\theta_2 - \theta_1) & K_2\cos(\theta_2 - \theta_1) & -3a\omega_1^2 + K_1 & 0 \\ K_2\cos(\theta_2 - \theta_1) & -K_2\cos(\theta_2 - \theta_1) & 0 & -3a\omega_1^2 + K_1 \end{bmatrix}$$

$$A_{(z_1)} = \frac{\partial f}{\partial z} = \begin{bmatrix} 0 & 0 & 1 & 0 \\ 0 & 0 & 0 & 1 \\ -K_2 & K_2 & K_1 & 0 \\ K_2 & -K_2 & 0 & K_1 \end{bmatrix}$$

The eigenvalues of A are calculated and given below:

$$\lambda_1 = 0$$

$$\lambda_2 = K_1$$

$$\lambda_3 = \frac{K_1}{2} - \frac{\sqrt{(K_1^2 - 8K_2)}}{2}$$

$$\lambda_4 = \frac{K_1}{2} + \frac{\sqrt{(K_1^2 - 8K_2)}}{2}$$

For z_1 to be an unstable focus, $K_1 > 0$ and $K_1^2 - 8K_2 < 0$ which is achieved when $K_2 > \frac{K_1^2}{8}$, should be satisfied.

For $K_1 > 0$ and $K_2 > \frac{K_1^2}{8}$ then z_2 and z_3 are saddle points and since $z_1 \in \Omega$ then by poincare bendixon criterion there is a periodic orbit around z_1. Since equilibrium point z_1 corresponds to the synchronized formation by having $\theta_1 = \theta_2$, a periodic orbit around z_1 corresponds to having the fish moving in the same direction while not having the same heading at each time t. Therefore, fish move in parallel.

Now consider the case of arbitrary N vehicles. in order for the vehicles to move in parallel, the equilibrium point corresponding to $\theta_i = \theta_j$ for all $i, j \in N$ should be an unstable focus and all other equilibrium points should be saddle. In order to achieve this, I have to find the eigenvalues of the jacobian of system (5.1) around the equilibrium point corresponding to $\theta_i = \theta_j$ for all $i, j \in N$. Let's call that point z_1'.

Using matlab symbolic toolbox, the eigenvalues of the jacobian around z_1' are given below:

$$\lambda_1 = 0$$

$$\lambda_2 = K_1$$

$$\lambda_3 = \frac{K_1}{2} - \frac{\sqrt{(K_1^2 - 4NK_2)}}{2}$$

$$\lambda_4 = \frac{K_1}{2} + \frac{\sqrt{(K_1^2 - 4NK_2)}}{2}$$

$$\vdots$$

$$\lambda_{N*N-1} = \frac{K_1}{2} - \frac{\sqrt{(K_1^2 - 4NK_2)}}{2}$$

$$\lambda_{N*N} = \frac{K_1}{2} + \frac{\sqrt{(K_1^2 - 4NK_2)}}{2}$$

A clear observation is that all of the eigenvalues are identical to λ_3 and λ_4 except λ_1 and λ_2.

Hence to achieve parallel formation, $K_1 > 0$ and $K_1^2 - 4NK_2 < 0$ which is achieved when $K_2 > \frac{K_1^2}{4N}$,should be satisfied. Similarly , all of the other equilibrium points are saddle under the previous conditions. Since equilibrium point z_1' corresponds to the synchronized formation by having $\theta_1 = \theta_2 = \cdots = \theta_N$, a periodic orbit around z_1' corresponds to having the fish moving in the same direction while not having the same heading at each time t. Therefore, fish move in parallel for arbitrary N and proof is completed.

□

The previous analysis is illustrated by simulating the closed loop Chaplygin sleigh fish robot system with the parameters listed in table (5.1). For $N = 8$ fish initialized with random heading in the range of [0 π] and zero velocity and angular rate. Since the

previous analysis applies to the approximate Chaplygin sleigh dynamics, I simulate the full dynamics with the closed loop form of the system (5.1) The Fig.(5.1-b) shows all N fish converging to the same limit cycle in the (v, ω) and (v, ω) planes. As a result, all of the fish robots move in the same direction in parallel as shown in Fig.(5.1-c)

5.2 Circular Formation Control

In section (3.2), I was able to achieve circular motion for a single fish. I was also able to estimate the approximate radius of the circle on which the fish moves (3.19). In this section, I extend the approach used in (3.2) to incorporate circular formation of multiple identical fish.

Consider a collective of N Chaplygin sleighs, with each sleigh labeled with an index k or j from the set $\mathcal{N} \triangleq \{1, \ldots, N\}$. by choosing

$$u_k = b(-K_1\omega_k - K_2 \sin(\theta_d - \theta_k) - K_3 \frac{l}{d}\omega_0(\omega_k - \omega_0^{-1})\langle L_k \boldsymbol{c}, e^{i\theta_k}\rangle \ ,$$

Where $\boldsymbol{c} = [c_1, ..., c_n]$, $c_k = r_k + i\omega_0^{-1}e^{i\theta_k}$ and $\omega_0^{-1} = \frac{\frac{bk_1}{ml}}{\omega_d}$ given by (3.19). Hence the

Parameter	**Symbol**	**Value**
Mass	m	1.4 kg
Length	l	0.31 m
Drag coefficient	d	0.5
Moment of inertia	b	0.1395 kg·m^2
Control gains	(K_1, K_2)	$(0.5, 2)$

Table 5.1: Parameters used to simulate the closed-loop fish-robot system (5.1)

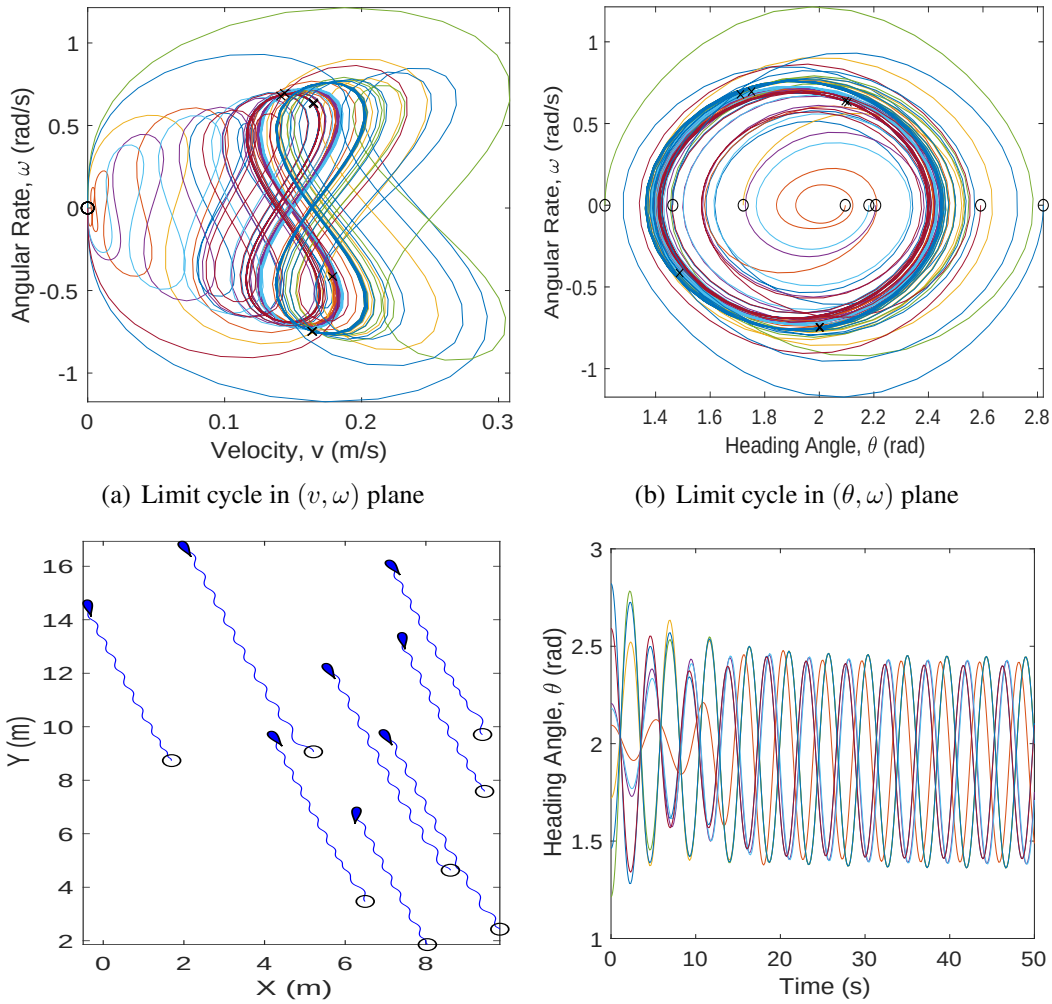

(a) Limit cycle in (v, ω) plane

(b) Limit cycle in (θ, ω) plane

(c) Paths in the (x, y) plane

(d) Heading angle time history

Figure 5.1: Simulation of the closed loop system (5.2) with $N = 8$ identical fish

system (3.1) becomes:

$$\begin{aligned}
\dot{v}_k &= l\omega^2 - dv_k \\
\dot{\theta}_k &= \omega_k \\
\dot{\omega}_k &= -\frac{ml}{b} v_k \omega_k + K_1 \omega_k + K_2 \sin(\theta_d - \theta) - K_3 \frac{l}{d} (\omega_k - \omega_0^{-1}) \langle L_k \boldsymbol{c}, e^{i\theta_k} \rangle
\end{aligned} \tag{5.4}$$

The system (5.4) can be divided into a slow and fast subsystems [33]. The fast v

subsystem can be written as

$$\dot{v} = d\left(\frac{l}{d}\omega^2 - v\right) \ . \tag{5.5}$$

For d sufficiently large, this subsystem converges to $v = \frac{l}{d}\omega^2$. Let $a = \frac{ml^2}{bd} > 0$. With the substitution $v = \frac{l}{d}\omega^2$, the slow (θ, ω) subsystem becomes:

$$\begin{aligned} \dot{\theta_k} &= \omega_k \\ \dot{\omega_k} &= -a\omega_k^3 + K_1\omega_k + K_2\sin(\theta_d - \theta) - K_3\frac{l}{d}(\omega_k - \omega_0^{-1})\langle L_k\boldsymbol{c}, e^{i\theta_k}\rangle, \end{aligned} \tag{5.6}$$

By changing the coordinates of the system (5.6) from (ω, θ) to (ω, γ), (5.6) becomes:

$$\begin{aligned} \dot{\gamma_k} &= \omega_k - \omega_d \\ \dot{\omega_k} &= -a\omega_k^3 + K_1\omega_k - K_2\sin(\gamma) - K_3\frac{l}{d}(\omega_k - \omega_0^{-1})\langle L_k\boldsymbol{c}, e^{i\gamma_k + \theta_d}\rangle \end{aligned} \tag{5.7}$$

Proposition 7. *solutions of the the closed loop control (5.7) are trapped in the set* $\Omega = \{\|\omega_k\| < \sqrt{\frac{K_1 + \sqrt{K_1^2 + 4a|\omega_d|}}{2a}}\}$

Proof. let

$$V = \frac{1}{2}\boldsymbol{\omega^T\omega} + \sum_{k=1}^{N} K_2[1 - \cos\gamma] + \frac{K_3}{2}\boldsymbol{c}^T L\boldsymbol{c}$$

by taking the derivative of V along the system (5.7) I get:

$$
\begin{aligned}
\dot{V} &= \sum_{k=1}^{N}[\dot{\omega_k}\omega_k + (\omega_k - \omega_d)\sin(\gamma_k)] \\
&= \sum_{k=1}^{N}[-a\omega_k^4 + K_1\omega_k^2 - K_2\omega_k\sin(\gamma_k) + K_2\omega_k\sin(\gamma) - K_2\omega_d\sin(\gamma_k)] \\
&- \sum_{k=1}^{N}[\frac{l}{d}\omega_k K_3(\omega_k - \omega_0^{-1})\langle L_k\boldsymbol{c}, e^{i(\gamma_k+\theta_d)}\rangle] + \sum_{k=1}^{N}[K_3\langle L_k\boldsymbol{c}, \dot{c}_k\rangle] \\
&= \sum_{k=1}^{N}[-a\omega_k^4 + K_1\omega_k^2 - K_2\omega_d\sin(\gamma_k)] \\
&- \sum_{k=1}^{N}\frac{l}{d}\omega_k K_3(\omega_k - \omega_0^{-1})\langle L_k\boldsymbol{c}, e^{i(\gamma_k+\theta_d)}\rangle + \sum_{k=1}^{N}K_3\langle L_k\boldsymbol{c}, v_k e^{i(\gamma_k+\theta_d)} - \omega_0^{-1}\omega_k e^{i(\gamma_k+\theta_d)}\rangle \\
&= \sum_{k=1}^{N}[-a\omega_k^4 + K_1\omega_k^2 - K_2\omega_d\sin(\gamma_k)] - \sum_{k=1}^{N}\frac{l}{d}\omega_k K_3(\omega_k - \omega_0^{-1})\langle L_k\boldsymbol{c}, e^{(i\gamma_k+\theta_d)}\rangle \\
&+ \sum_{k=1}^{N}K_3\langle L_k\boldsymbol{c}, \frac{l}{d}\omega_k^2 e^{(i\gamma_k+\theta_d)} - \omega_0^{-1}\omega_k e^{(i\gamma_k+\theta_d)}\rangle \\
&= \sum_{k=1}^{N}-a\omega_k^4 + K_1\omega_k^2 - K_2\omega_d\sin(\gamma_k) - \sum_{k=1}^{N}\frac{l}{d}\omega_k K_3(\omega_k - \omega_0^{-1})\langle L_k\boldsymbol{c}, e^{i(\gamma_k+\theta_d)}\rangle \\
&+ \sum_{k=1}^{N}K_3\frac{l}{d}\omega_k(\omega_k - \omega_0^{-1})\langle L_k\boldsymbol{c}, e^{i(\gamma_k+\theta_d)}\rangle \\
&= \sum_{k=1}^{N}[-a\omega_k^4 + K_1\omega_k^2 - K_2\omega_d\sin(\gamma_k)] \\
&\leq \sum_{k=1}^{N}[-a\omega_k^4 + K_1\omega_k^2 + K_2|\omega_d|]
\end{aligned}
\tag{5.8}
$$

Following the same analysis of section 3.2, when $\|\omega_k\| > \sqrt{\frac{K_1+\sqrt{K_1^2+4a|\omega_d|}}{2a}}$, $\dot{V} \leq 0$

Also, for $\|\omega_k\| = \sqrt{\frac{K_1+\sqrt{K_1^2+4a|\omega_d|}}{2a}}$, the time derivative of V is $\dot{V} \leq 0$, therefore the set $\Omega = \{\|\omega_k\| < \sqrt{\frac{K_1+\sqrt{K_1^2+4a|\omega_d|}}{2a}}\}$ is positively invariant and solutions of (5.7) are trapped in Ω which completes the proof.

□

Remark 8. *In order to prove that the fish move around the same circle, the equilibrium points of (5.7) that correspond the* $c_k = c_j$,$\omega_k = \omega_d$ *and* $\gamma_k = 0$ *for all* $k, j \in \mathcal{N}$ *must be an unstable focus.*

Simulation of the closed loop system (5.4) using the parameters provided in Table (3.2) with $\omega_d = 0.2rad/s, K_1 = 0.5, K_2 = 2$, $K_3 = 0.1$ and for $N = 8$ fish is provided in Fig (5.2). The mean of each centre of motion of the $N = 8$ fish is plotted too in (c). it is clear that all of the fish robots move around the same centre on average.

By changing θ_d to $\theta_d = \omega_d t + \theta_k(0)$ in system (5.4) where the spacing between $\theta_k(0)$ is set to be symmetric, a swarm of fish moving around the same circle is obtained. These fish have the same radius and exhibit a symmetric formation.

Symmetric formation is provided in Fig (5.2) where each arrow on each agent points the phase orientation of each fish.

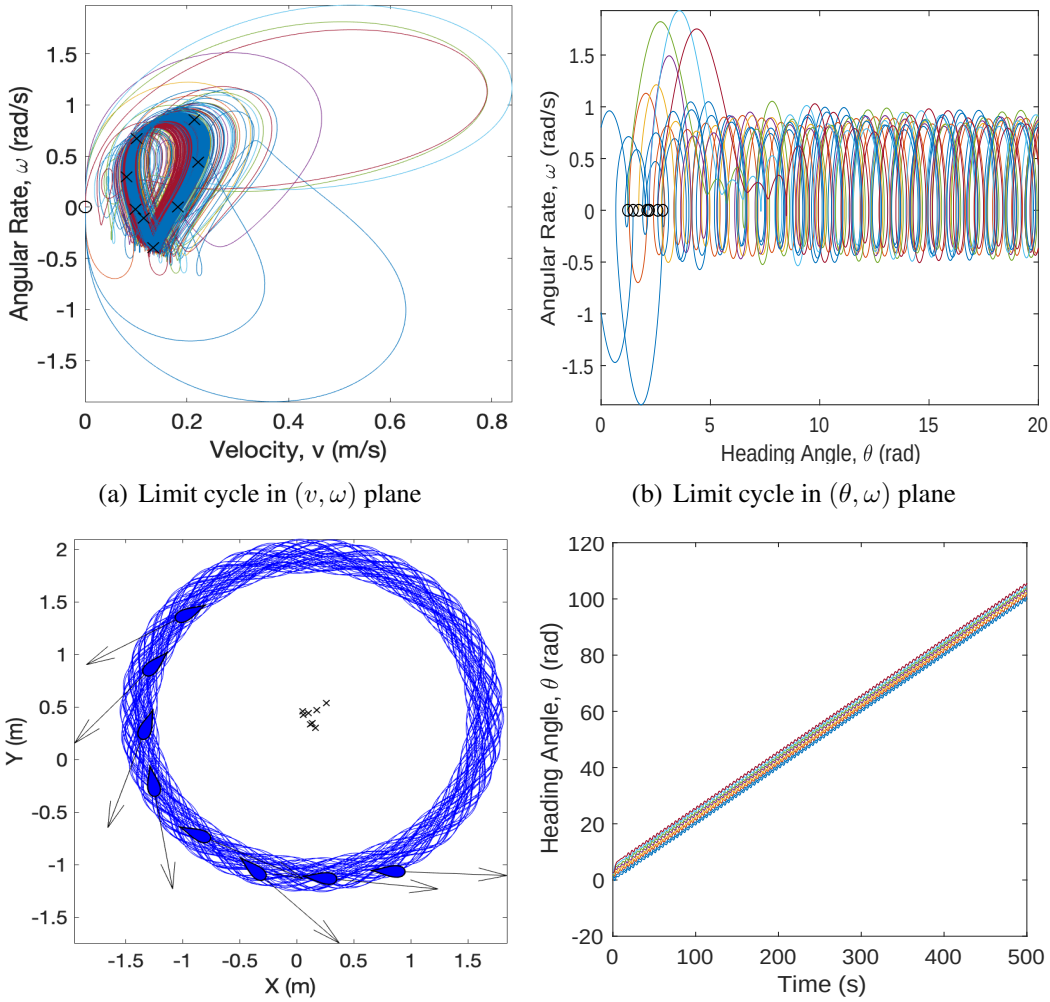

(a) Limit cycle in (v, ω) plane

(b) Limit cycle in (θ, ω) plane

(c) Paths in the (x, y) plane

(d) Heading angle time history

Figure 5.2: simulation of the closed loop system (5.4) with $N = 8$ identical fish

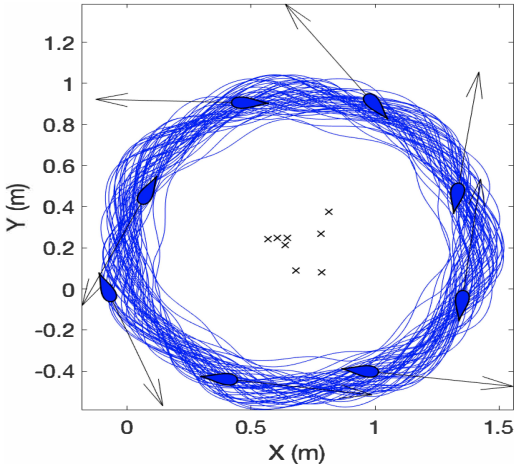

Figure 5.3: Simulation of closed loop system (5.4) with N=8 and with symmetric desired heading. the arrows on each particle represent the phase of each one of them.

Chapter 6: Conclusion

6.1 Summary of Contributions

This thesis presents a novel cooperative control law that achieves second-order consensus, parallel and circular formations with nonlinear dynamics of N identical vehicles on the tangent bundle of $\mathbb{T}^N$. The proposed feedback control relies either on velocity measurement between agents or heading of each agent where communication does not have to be all-to-all. It does not include feedback linearization of the agents' dynamics. Furthermore, the consensus and formation control law are achieve while maintaining the flapping of the N fish which was not considered from previous consensus and formation algorithms. We examine our control law on a simulated school of N robotic fish. The control laws synchronize the motion of the fish in the desired direction, achieve parallel formation control without using any desired heading and also circular formation.

6.2 Suggestions for Ongoing and Future Work

In ongoing work, I seek to drive the N vehicles in a circular motion while synchronizing their phases. Also, I would like to explore circular formation with symmetric phase arrangements so all of the fish would move on the same circle while having symmetric

phases.

In addition, since this thesis assumes identical vehicles, it is crucial in future work to consider different fish dynamics, or same dynamics but with modeling error in order to incorporate the reality that all of the fish cannot be identical. Similarly, signal noise and communication delay between the fish should be incorporated because this paper does not consider that the measured states have noise nor communication delays.

Finally, experimental validation of these simulation should be done for at least N=2 fish.

Bibliography

[1] W. Ren, R. W. Beard, and E. M. Atkins, "Information consensus in multivehicle cooperative control," *IEEE Control Systems Magazine*, vol. 27, no. 2, pp. 71–82, 2007.

[2] C. W. Reynolds, *Flocks, herds and schools: A distributed behavioral model*. Association for Computing Machinery, 1987, vol. 21, no. 4.

[3] T. Vicsek, A. Czirook, E. Ben-Jacob, O. Cohen, and I. Shochet, "Novel type of phase transition in a system of self-driven particles," *Physical Review Letters*, vol. 75, pp. 1226–1229, 1995.

[4] H. Shi, L. Wang, and T. Chu, "Flocking of multi-agent systems with a dynamic virtual leader," *International Journal of Control*, vol. 82, pp. 43–58, 2009.

[5] R. Olfati-Saber and R. M. Murray, "Graph rigidity and distributed formation stabilization of multi-vehicle systems," in *IEEE Conference on Decision and Control*, 2002, pp. 2965–2971.

[6] Y. Hong, G. Chen, and L. Bushnell, "Distributed observers design for leader-following control of multi-agent networks," *Automatica*, vol. 44, no. 3, pp. 846–850, 2008.

[7] Y. Cao, W. Yu, W. Ren, and G. Chen, "An overview of recent progress in the study of distributed multi-agent coordination," *IEEE Transactions on Industrial Informatics*, vol. 9, no. 1, pp. 427–438, 2013.

[8] L. Sabattini, C. Secchi, N. Chopra, and A. Gasparri, "Distributed control of multirobot systems with global connectivity maintenance," *IEEE Transactions on Robotics*, vol. 29, no. 5, pp. 1326–1332, 2013.

[9] W. Ren, "Multi-vehicle consensus with a time-varying reference state," *Systems & Control Letters*, vol. 56, no. 7-8, pp. 474–483, 2007.

[10] Y. Cao, W. Ren, and Y. Li, "Distributed discrete-time coordinated tracking with a time-varying reference state and limited communication," *Automatica*, vol. 45, no. 5, pp. 1299–1305, 2009.

[11] W. Ren and R. W. Beard, "Consensus seeking in multiagent systems under dynamically changing interaction topologies," *IEEE Transactions on Automatic Control*, vol. 50, no. 5, pp. 655–661, 2005.

[12] L. Moreau, "Stability of multiagent systems with time-dependent communication links," *IEEE Transactions on Automatic Control*, vol. 50, no. 2, pp. 169–182, 2005.

[13] Y. Cao and W. Ren, "Finite-time consensus for single-integrator kinematics with unknown inherent nonlinear dynamics under a directed interaction graph," in *American Control Conference*, 2012, pp. 1603–1608.

[14] S. E. Tuna, "Conditions for synchronizability in arrays of coupled linear systems," *IEEE Transactions on Automatic Control*, vol. 54, no. 10, pp. 2416–2420, 2009.

[15] N. Chopra, "Output synchronization on strongly connected graphs," *IEEE Transactions on Automatic Control*, vol. 57, no. 11, pp. 2896–2901, 2012.

[16] T. Li, M. Fu, L. Xie, and J.-F. Zhang, "Distributed consensus with limited communication data rate," *IEEE Transactions on Automatic Control*, vol. 56, no. 2, pp. 279–292, 2011.

[17] R. A. Horn and C. R. Johnson, *Matrix Analysis*. Cambridge University Press, 1990.

[18] Y. Zhang and Y.-P. Tian, "Consentability and protocol design of multi-agent systems with stochastic switching topology," *Automatica*, vol. 45, no. 5, pp. 1195–1201, 2009.

[19] W. Ren, "On consensus algorithms for double-integrator dynamics," *IEEE Transactions on Automatic Control*, vol. 53, no. 6, pp. 1503–1509, 2008.

[20] H. Su, G. Chen, X. Wang, and Z. Lin, "Adaptive second-order consensus of networked mobile agents with nonlinear dynamics," *Automatica*, vol. 47, no. 2, pp. 368–375, 2011.

[21] W. Yu, G. Chen, M. Cao, and J. Kurths, "Second-order consensus for multiagent systems with directed topologies and nonlinear dynamics," *IEEE Transactions on Systems, Man, and Cybernetics, Part B (Cybernetics)*, vol. 40, no. 3, pp. 881–891, 2010.

[22] L. Scardovi, A. Sarlette, and R. Sepulchre, "Synchronization and balancing on the N-torus," *Systems & Control Letters*, vol. 56, no. 5, pp. 335–341, 2007.

[23] A. Sarlette and R. Sepulchre, "Consensus optimization on manifolds," *SIAM Journal on Control and Optimization*, vol. 48, no. 1, pp. 56–76, 2009.

[24] S. Nair and N. E. Leonard, "Stable synchronization of rigid body networks," *Networks and Heterogeneous Media*, vol. 2, no. 4, p. 597, 2007.

[25] D. A. Paley, "Stabilization of collective motion on a sphere," *Automatica*, vol. 45, no. 1, pp. 212–216, 2009.

[26] R. Dong and Z. Geng, "Consensus based formation control laws for systems on Lie groups," *Systems & Control Letters*, vol. 62, no. 2, pp. 104–111, 2013.

[27] R. Sepulchre, D. A. Paley, and N. E. Leonard, "Stabilization of planar collective motion: All-to-all communication," *IEEE Transactions on Automatic Control*, vol. 52, no. 5, pp. 811–824, 2007.

[28] E. W. Justh and P. Krishnaprasad, "Equilibria and steering laws for planar formations," *Systems & Control Letters*, vol. 52, no. 1, pp. 25–38, 2004.

[29] J. A. Acebrón, L. L. Bonilla, C. J. P. Vicente, F. Ritort, and R. Spigler, "The Kuramoto model: A simple paradigm for synchronization phenomena," *Reviews of Modern Physics*, vol. 77, no. 1, p. 137, 2005.

[30] F. Dörfler and F. Bullo, "Synchronization in complex networks of phase oscillators: A survey," *Automatica*, vol. 50, no. 6, pp. 1539–1564, 2014.

[31] R. Sepulchre, D. A. Paley, and N. E. Leonard, "Stabilization of planar collective motion with limited communication," *IEEE Transactions on Automatic Control*, vol. 53, no. 3, pp. 706–719, 2008.

[32] S. Napora and D. A. Paley, "Observer-based feedback control for stabilization of collective motion," *IEEE Transactions on Control Systems Technology*, vol. 21, no. 5, pp. 1846–1857, 2013.

[33] J. Lee, S. Santana, B. Free, and D. A. Paley, "State-feedback control of an internal rotor for propelling and steering a flexible fish-inspired underwater vehicle," accepted for presentation at the *2019 American Control Conference*.

[34] S. D. Kelly, M. J. Fairchild, P. M. Hassing, and P. Tallapragada, "Proportional heading control for planar navigation: The Chaplygin beanie and fishlike robotic swimming," in *American Control Conference*, 2012, pp. 4885–4890.

[35] R. Diestel, "The basics," in *Graph Theory*. Springer, 2000, pp. 1–28.

[36] H. Schattler and U. Ledzewicz, "An Introduction to Differentiable Manifolds," in *Geometric Optimal Control: Theory, Methods and Examples*. Springer, 2012, pp. 593–614.

[37] D. A. Paley, "Cooperative control of an autonomous sampling network in an external flow field," in *2008 47th IEEE Conference on Decision and Control*. IEEE, 2008, pp. 3095–3100.

[38] P. Tallapragada and S. D. Kelly, "Self-propulsion of free solid bodies with internal rotors via localized singular vortex shedding in planar ideal fluids," *The European Physical Journal Special Topics*, vol. 224, no. 17-18, pp. 3185–3197, 2015.

[39] P. Tallapragada and V. Fedonyuk, "Steering a chaplygin sleigh using periodic impulses," *Journal of Computational and Nonlinear Dynamics*, vol. 12, no. 5, p. 054501, 2017.

[40] H. K. Khalil, "Advanced stability analysis," in *Nonlinear Systems*. Prentice Hall, 2002.